IOP Conf. Series: Materials Science and Engineering **375** (2018) 012005 doi:10.1088/1757-899X/375/1/012005

About the combined role of texture and grain size on hardening behavior of cp titanium sheets

F. Wagner[1,2], T. Richeton[1,2], C. Chen[1,3] and L.S. Toth[1,2]

[1] Labex DAMAS, Université de Loraine, France
[2] LEM3 CNRS (UMR 7239) - Université de Lorraine, Metz, France
[3] now at Nanjing University of Science and Technology, China
E-mail: francis.wagner@univ-lorraine.fr

Abstract. The goal of the study is to analyze the role of both the grain size distribution and the crystallographic texture on the plastic deformation. Data consist, on one hand, in tensile curves obtained for commercially pure titanium samples elaborated to correspond at several mean grain sizes and textures. Data consist, on the other hand, in calculated tensile curves using a crystal plasticity EVPSC model modified to include grain size effects. The trend for the yield stresses and the initial plateaus are satisfying showing that the effects of grain size are captured in the model. Under the conditions used in the model the hardening is however not enough grain size dependent when compared with experiments.

1. Introduction

Since decades the plastic deformation of polycrystalline materials has been studied from a very large number of experiments as well as from many model calculations [1, 2] in order to understand in details the mechanisms which govern this deformation and to have predictive tools. It was recognized very soon that the texture is a key factor for the plastic behavior. Although known at the macroscopic level (Hall-Petch relationship for example), the role of the mean grain size and the grain size distribution have attracted less attention. Only few papers consider the effects of both texture and grain size distribution on the mechanical behavior (e.g., [3-8]). The goal of the present paper is to contribute to a better understanding of the combined role of crystallographic texture and grain size during plastic deformation. For that purpose a set of specimens showing various microstructures was prepared, characterized using a FEG-SEM (with EBSD) and then submitted to tensile tests. The used material was cp (commercially pure) titanium (grade 2). On the other hand a crystal plasticity model, EVPSC (elasto-visco-plastic self-consistent) type [9], was modified to include grain size effects. The comparison of the experimental and simulated results was used to clarify the respective role of the texture and grain size.

2. Materials and experiments

2.1 Preparation of the specimens

The as-received material was a 2 mm-thick plate of commercially pure titanium (Ti grade 2 or T40 according to TIMET*) in a fully recrystallized state with a mean grain size of about 10 µm. Specimens cut off from this plate were cold rolled, most of the time along the previous RD (Rolling Direction) and in a few cases along the previous TD (Transverse Direction). After the deformation, the specimens were annealed under various conditions in a furnace working under secondary vacuum. The conditions of preparation for the seven selected specimens used in this study are reported in Table 1. The specimens had a dog bone shape (total length 43 mm) and could be put entirely in a FEG-SEM.

2.2 Microstructural characterization of the specimens

The microstructural characterization of these specimens was made by using EBSD maps. An example of such maps is presented at Figure 1. From each EBSD map a set of grains was extracted. The size and the orientation of each grain were determined using a post-processing software (Chanel 5* or JTEX*). D_m, in Table 1, is the mean grain size. In all the cases the specimens were fully recrystallized.

Table 1: List of the seven specimens, their preparation conditions, some metallurgical data and some mechanical characteristics (the quantities related to mechanical properties are defined in section 2.4)

Specimen name	Cold rolling reduction	Rolling direction	Annealing conditions	Number of grains	D_m (µm)	σ_e (MPa)	LP1 (%)	σ_{max} MPa	ε* (%)
R_2.8	75%	// RD	500°C–40mn	6254	2.8	390	2.1	485	21.7
T_2.8	75%	// TD	500°C–40mn	7328	2.8	383	4.7	436	22.3
R_4.8	75%	// RD	650°C – 1 h	8793	4.8	331	1.0	442	16.4
RR_9.8	75%	// RD	730°C – 2 h	3262	9.8	354	-	494	14.6
RT_9.8	75%	// RD	730°C – 2 h	3262	9.8	375	2.0	440	9.7
R_11.7	75%	// RD	740°C – 2 h	4075	11.7	353	-	466	18.4
R_21.3	30%	// RD	840°C – 4 h	1273	21.3	282	-	484	18.8

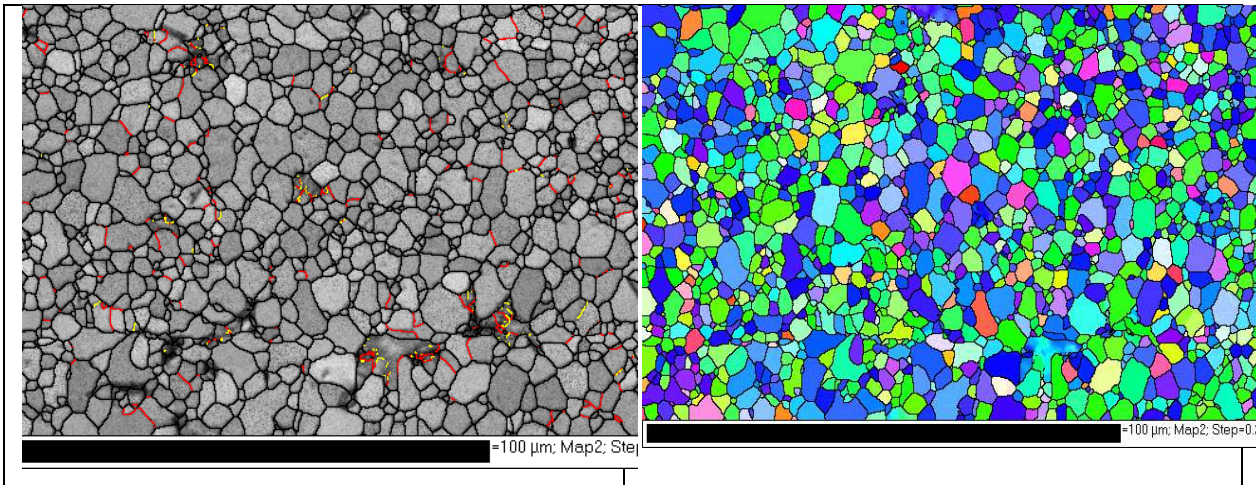

a) BC (Band Contrast) map **b)** IP (Inverse Pole) map

Figure 1: Part of an EBSD map for the specimen R_2.8 (mean grain size D_m=2.8 µm)
a) BC map b) IP map for the direction RD

The specimens with the smallest grains were close to the end of the primary recrystallization. Note that the number in the names of the specimens (Table 1) refers to the mean grain size in microns. For the two specimens with a mean grain size 9.8 µm, the notations used in Table 1 distinguish the case rolling // RD and extension // RD (sample RR_9.8) from the case rolling // RD and extension // TD (sample RT_9.8).

2.3 Texture

For each specimen the data set of the grains (size and orientation) was used to calculate the ODF. An example is given at figure 2 where the section Phi1=0° is presented for two specimens. The ODF's correspond to well known textures for this material [10, 11]. When the grains are small, which means that the annealing was stopped close to the end of the primary recrystallization, the texture resembles the deformation one whereas the 'grain growth texture' is obtained after heat treatments made at higher temperatures (see [12] for further information).

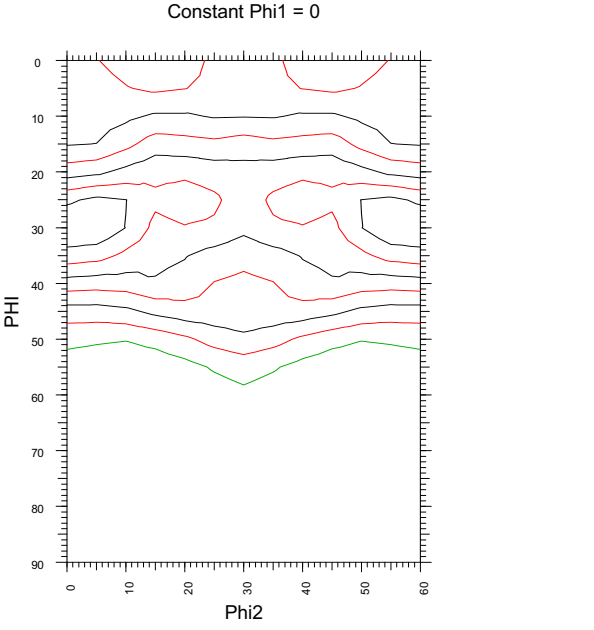

a) Sample R_2.8
Contour levels: 1., 2., 3., 4., 5., 6., 7.

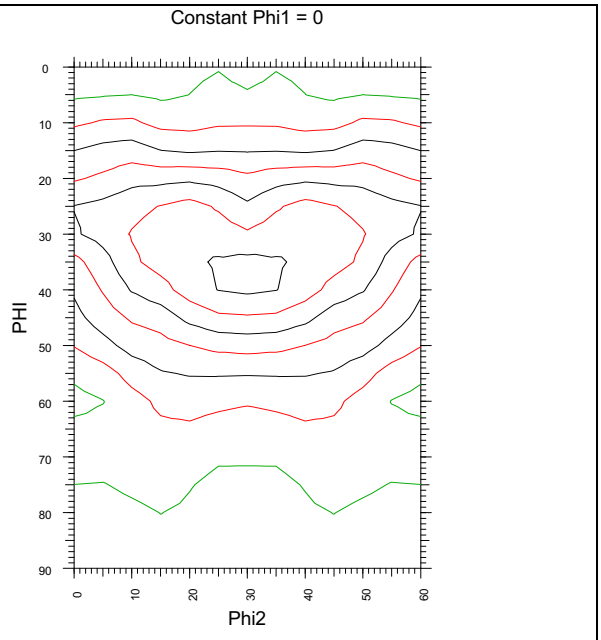

b) Sample R_11.7
Contour levels: 1., 2., 3., 4., 5., 6., 7.

Figure 2: Section Phi1=0° of the ODF for two specimens a) sample R_2.8 b) sample R_11.7

For the simulations which are shown later on, the data consist in a list of grains with, for each one, its orientation (Euler angles) and its grain diameter *Dg*.

2.4 Mechanical characterization

The samples were small dog-bone-shaped specimens (total length L_0=43 mm, gauge length L_g=11.0 mm, width w_0=3.0 mm, thickness t_o=0.5 mm). Tensile tests were conducted at ambient temperature on a Deben Microtest MT10331-1kN tensile machine at a constant displacement speed of 0.5mm/mn which corresponds to an initial strain rate of 7.5 10^{-4} s^{-1}. The extension direction was parallel to the last rolling direction except for the sample RT_9.7 (extension direction // TD). An example of the tensile curves is shown at Figure 3.

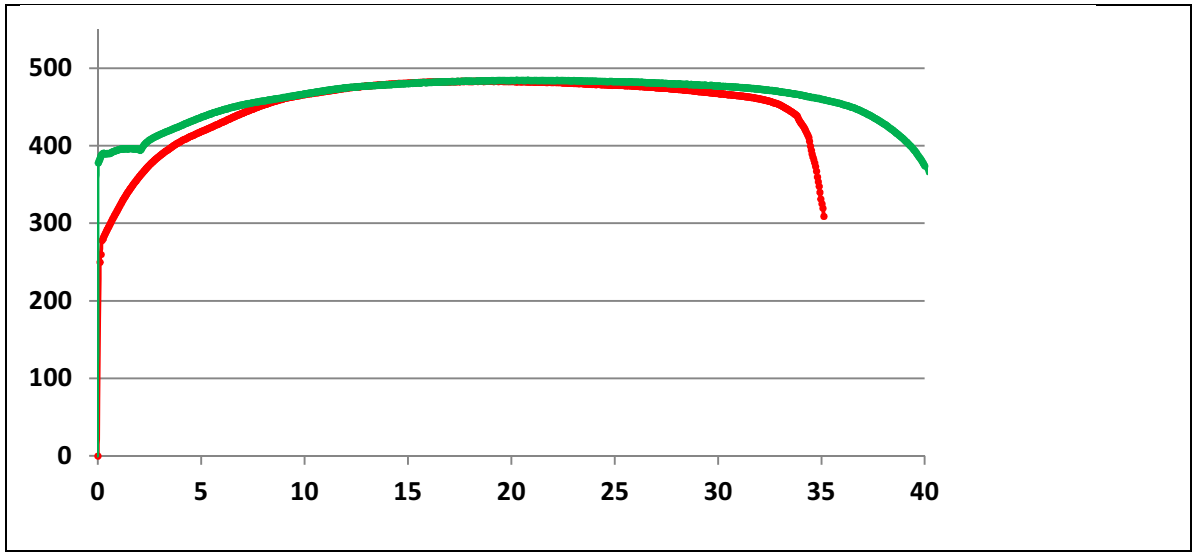

Figure 3: Engineering stress (MPa), σ_eng, versus engineering strain in %, ε_eng, for the two specimens R_21.3 (red curve) and R_2.8 (green curve).

Several quantities were extracted from the tensile curves to characterize (and discuss in the followings) the mechanical behavior: σ_e is the yield stress, LP1 stands for the length (in %) of the first plateau which appears sometimes in the beginning of the plastic deformation, σ_{max} is the maximal engineering stress, ε* is the corresponding engineering strain (in %). These values are reported in Table 1. We will use also further on the quantity $\Delta\sigma = \sigma_{max} - \sigma_e$ to characterize the 'hardening amplitude'.

From these experiments two trends were remarked:

i) the yield stress increases with decreasing grain size and follows rather well a Hall-Petch relationship [9, 10],
ii) the 'hardening amplitude', Δσ, tends to decrease with decreasing grain size [9].

3. Used model

3.1 Characteristics of the model

The model used to simulate the tensile behavior is the one that was developed in reference [13] to study hardening mechanisms in cp Ti. It is an EVPSC model based on an affine linearization of the viscoplastic flow rule and the translated fields technique to formulate the 1-site self-consistent

approximation [9]. At the level of the single crystal, glide on prismatic, basal, pyramidal <a>, 1st order pyramidal <c+a> and 2nd order pyramidal <c+a> is considered but not twinning. The slip rates $\dot{\gamma}^{(s)}$ result from the Orowan relation where the evolution of mobile dislocation densities and dislocation velocities are treated separately on each slip system. This allows to account for an initial fast multiplication of mobile dislocations. It was shown that this setting, together with the consideration of lower strain-rate sensitivity for prismatic systems, succeeded to reproduce the three-stage hardening behavior of cp Ti in tensile conditions.

3.2 Taking into account the effects of grain size

In order to take into account grain size effects in the model, two modifications were made in the constitutive laws. Following references [3-8], the assumption was made that the critical resolved shear stresses (crss) $\tau_c^{(s)}$ depends on the *individual grain size* D_g in a Hall-Petch type relationship:

$$\tau_c^{(s)} = \tau_0^{(s)} + \mu^{(s)} b^{(s)} \sqrt{\sum_l a^{(sl)} \rho_f^{(l)}} + \frac{k_1^{(s)}}{\sqrt{D_g}} \qquad (1)$$

In this formula, *s* or *l* designates the slip system, $\tau_0^{(s)}$ the lattice friction stress, $\mu^{(s)}$ the directional shear modulus, $b^{(s)}$ the Burgers vector magnitude, $a^{(sl)}$ interaction coefficients between systems, $\rho_f^{(l)}$ forest (or sessile) dislocation density that increases with plastic deformation and $k_1^{(s)}$ that is thus a Hall-Petch type slope resolved on the slip system. Note that with this supplementary Hall-Petch -type term, the crss are different *from grain to grain* according to their size, the smallest grains being harder that the largest ones.

The second modification made was based on the idea that, with decreasing grain size, i.e. with increasing ratio grain boundary area over grain volume, the balance between dislocation absorption and emission at grains boundaries is changed in favor of absorption. In order to account for this effect, the dynamic recovery term, which is present within the evolution equation of forest densities [13], was made grain size dependent as follows:

$$\dot{\rho}_f^{(s)} = \frac{1}{b^{(s)}} \left(\frac{1}{L^{(s)}} - 2k_c^{(s)} b^{(s)} \left(\rho_f^{(s)} + \frac{k_2^{(s)}}{D_g^2} \right) \right) \left| \dot{\gamma}^{(s)} \right| \qquad (2)$$

Through equations (1) and (2), it is seen that $k_2^{(s)}$, by influencing the evolution of the forest dislocation densities, will modify the hardening behavior. k_1 and k_2 were taken the same for all the slip systems. Their values are reported in Table 2 along with the values of $\tau_0^{(s)}$ and ρ_{f_0} (initial forest density). The other model's parameters are the same as in [13].

Table 2: List of the model's parameters.

k_1 (MPa.m$^{0.5}$)	k_2	ρ_{f_0} (m^{-2})	$\tau_0^{(s)}$ (MPa)				
			Prismatic	Basal	Pyr. <a>	1st order pyr. <c+a>	2nd order pyr. <c+a>
0.114	40	10^{12}	100	145	145	130	290

These crss values seem in accordance with some of the data reported in [14].

4. Results and discussion

Two examples of simulated tensile curve, compared to the experimental one, are shown at Figure4.

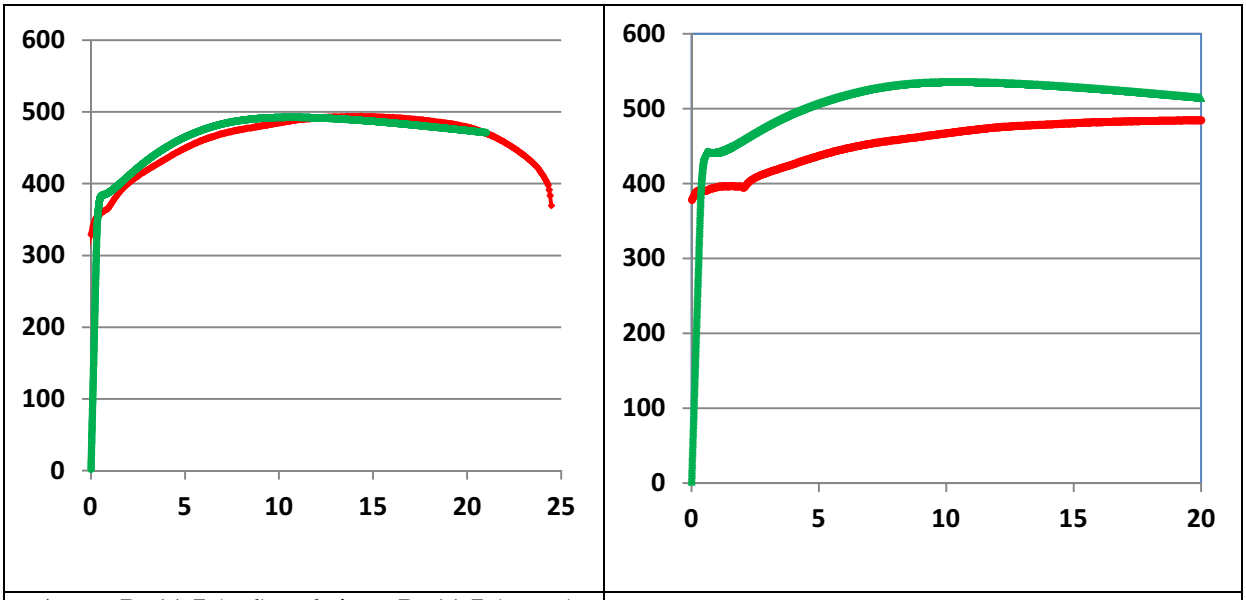

a) exp. R_11.7 (red) and simu. R_11.7 (green)

b) exp. R_2.8 (red) and simu. R_2.8 (green)

Figure 4: Experimental and simulated tensile curves (σ_eng (MPa) versus ε_eng (%))
a) sample R_11.7 b) sample R_2.8

4.1 Yield stress

The values of the yield stress for experiments and for simulations as function of the mean grain size are shown in Figure 5. The yield stresses calculated from the Hall-Petch relationship [9] are also plotted.

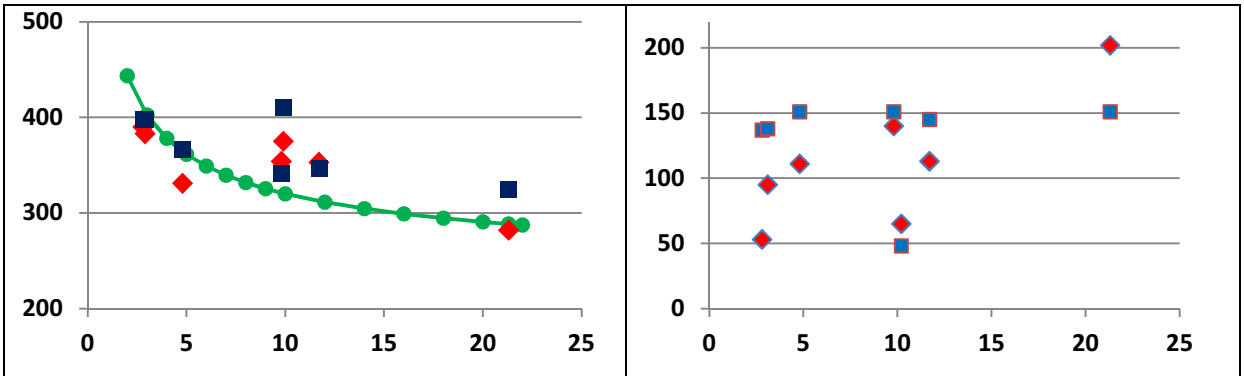

a) Yield stress (MPa) versus the grain size (µm); exp. red, simu. blue, HP green

b) Δσ, the 'hardening amplitude', (MPa) versus the grain size (µm); exp. red, simu. blue square

Figure 5: Comparison of experimental and calculated values of a) the yield stress b) $\Delta\sigma$ ($=\sigma_{max}-\sigma_e$)

The calculated yield stresses follow a correct trend which means that the assumption made for the dependence of the crss on the grain size (eq. 1) is relevant. The main discrepancy arises for the case where the tensile direction is parallel to TD (sample RT_9.8) due likely to crss which are somewhat too high for the pyramidal slips.

4.2 First plateau

When an initial plateau exists (see the values of LP1 in Table 1), the model reproduces it but somewhat shorter (see a typical example in Figure 4b). From the simulations, it is possible to analyze the activity of the several slip systems in the beginning of the plastic deformation. No plateau appears when the prismatic slip dominates. A plateau appears when there is a more balanced activity between prismatic, pyramidal <c+a> and pyramidal <a> slip systems. Under such conditions plastic strain incompatibilities and the induced internal stresses are strongly decreased. Along with the fast multiplication of mobile dislocations, this gives rise to an initial state with nearly no hardening.

4.3 Hardening

In all the cases the simulations reproduce correctly the three stages of the hardening rate $d\sigma/d\varepsilon$ which have been described in the literature for tensile experiments [13, 15, 16]. When considering the 'hardening amplitude', $\Delta\sigma$, it can be seen in Figure 5b that this quantity is nearly constant in the simulations whereas it increases with increasing grain size (except for the particular case of extension along TD – sample RT_9.8). This indicates that the term added in the model, eq. (2), by using a coefficient k_2=40, does not change enough the forest dislocation density rate. In order to produce a significant effect, one should use a much higher value of this coefficient. A simulation performed with k_2=1000, in a case with small grains (sample T_2.8), shows that $\Delta\sigma$ decreases strongly (from 137 MPa, with k_2=40, to 30 MPa). In the same time ε^*, the limit for homogeneous deformation, decreases somewhat and is smaller than the experimental value. This way to account for grain size effect in the hardening behavior should clearly be further calibrated.

5. Conclusion

By considering the tensile curves of a set of cp titanium specimens with several microstructures, especially with several mean grain sizes, it was recognized that the yield stress depends on the grain size following a Hall-Petch relationship. The 'hardening amplitude', defined as $\Delta\sigma = \sigma_{max} - \sigma_e$, shows also some dependence with the grain size. If a crystal plasticity model should account for such effects, it is necessary to include some 'internal length' in it. In this study, where a EVPSC model was used, it was made by adding a term that depends on the individual grain size, in a Hall-Petch manner, to the crss. The yield stresses obtained in the simulations reproduce rather correctly the experimental values, which validates up to some extent the assumption for the crss expression. The simulations lead to interpret the initial plateau, which sometimes appear in the beginning of the plastic deformation, in terms of combined slip activity compared to the dominant prismatic slip activity when no plateau arises. To account for the dependence of hardening on the grain size, a supplementary term was added in the evolution equation of the forest density dislocation. It is expected to amplify the dislocation absorption when the grain size decreases. The simulations show that the three stages for the hardening rate are correctly reproduces but that the 'hardening amplitude' is not enough sensitive to this supplementary term. A short test with a higher value of this term highlights that the parameter which governs the contribution of this term should be significantly increased to obtain more realistic results for the 'hardening amplitude'.

Acknowledgments: The authors thank Mr. Yvon Millet from the company Timet for providing cp Ti sheets and Dr. Laurent Peltier for performing various heat treatments. This work was supported by the French State through the program "Investment in the future" operated by the National Research Agency (ANR) and referenced by ANR-11-LABX-0008-01 (LabEx DAMAS).

References

[1] Kocks U F Tomé C N and Wenk H R **1998** Texture and Anisotropy, Cambridge University Press
[2] Roters F. Eisenlohr P Hantcherli L Tjahjanto D D Bieler T R and Raabe D **2010** *Acta Mat.* **58** p. 1152-1211
[3] Bunge H J Wagner Welch P I and Van-Houtte P **1985** *J. Phys. Lett.* **46** p.L1109-L1113.
[4] Sinclair C W Poole W J and Brechet Y **2006** *Scripta Mat,* **55** p.732-742
[5] Berbenni S Favier V and Berveiller M **2007** *Int. J. of Plasticty* **23** p.114-142
[6] Raeisinia B Sinclair C W Poole W J and Tomé C N **2008** *Mater. Sci. Eng*., **16,** p.1–15
[7] Fromm B S Adams B L Ahmadi S and Knezevic M X **2009** *Acta Mater* **57** p.2339-2348
[8] Nicaise N Berbenni S Wagner F Berveiller M and Lemoine X **2011** *Int. J. of Plasticity*, **27**, p.232-249
[9] Mareau C and Berbenni S **2015** *Int. J. of Plasticty* **64** p. 134-150
[10] Wagner F Bozzolo N Van Landuyt O and Grosdidier T **2002** *Acta Mat.* **50** p.1245-1259.
[11] Singh A K and Schwarzer R A **2008**, *Trans Indian Inst. Met.* **61** n°5 p.371-387.
[12] Wagner F Ouarem A Richeton T and Toth L S **2018**, to appear in *Adv. Eng. Mat*
DOI: 10.1002/adem.201700237
[13] Amouzou K E K Richeton T Roth A Lebyodkin M A Lebedkina T A **2016**, *Int. J. of Plasticity* **80** p. 222-240
[14] Wang L Zheng Z Phuka H Kenesei P Park J-S Lind J Suter R M and Bieler T R **2017** *Acta Mat.* **132** p.598-610
[15] H. Becker H and Pantleon W **2013** *Comput. Mater. Sci.* **76** p.52–59.
[16] Roth A Lebyodkin M A Lebedkina T A Lecomte J-S Richeton T and Amouzou K E K **2014** *Materials Science and Engineering A* **A596** p.236–243.